INTERNATIONAL JOURNAL OF AGRICULTURE & BIOLOGY
ISSN Print: 1560–8530; ISSN Online: 1814–9596
22–0383/2022/28–6–391–404
DOI: 10.17957/IJAB/15.1993
http://www.fspublishers.org

Full Length Article

The Possible Protective Effect of Luteolin in a Thioacetamide Rat Model of Testicular Toxicity

Sahar J. Melebary*
Department of Biology, College of Science, University of Jeddah, Jeddah 21493, Saudi Arabia
*For correspondence: Sjmelebary@uj.edu.sa
Received 03 September 2022; Accepted 19 November 2022; Published 12 December 2022

Abstract

Luteolin is a flavone that serves as a natural antioxidant. The therapeutic impacts of luteolin is influenced by its antioxidant, anti-inflammatory, anticancer, neuroprotective and antineoplastic properties. This study aimed to establish an animal model of testicular toxicity caused by Thioacetamide (TAA). In addition, high doses of Luteolin (LUT) were supplemented to observe the role of LUT in attenuating spermato-toxicity, the hazard of oxidative stress, and testicular histopathological alterations induced by TAA. Thirty adult rats were equally divided into three groups as follow; G1: negative control group, G2: was given TAA 200 mg/kg body weight, G3: was received LUT at a dose of (50 mg/kg body weight) for four weeks concurrently with TAA. During this experiment histological, immunohistochemical, biochemical and morphometric measures were evaluated. TAA revealed loss of normal architecture of testicular tissue, wide interstitial spaces, and a loss of stratal arrangement of germinal epithelium with intercellular spacing. Also, a reduction in the number of +ve vimentin staining Sertoli cells with a marked reduction in the mean of vimentin-positive cells increased oxidative stress in testicular tissue. LUT protected testis against these alterations. By reducing oxidative stress, histological and immunohistochemical alterations and restoring the normal testicular tissue architecture and function, LUT successfully lowers TAA testicular toxicity in albino rats, recommending that it may have similar effects in humans. © 2022 Friends Science Publishers

Keywords: Luteolin; Thioacetamide; Testicular Toxicity; Histological; Immunohistochemical

Introduction

The incidence of infertility has increased in recent years. Among all infertile couples, the proportion of infertility caused by male factors accounts for about 50% and affects one man in 20 in the general population (Agarwal *et al.* 2020). One of the proposed mechanisms for idiopathic infertility is oxidative stress (OS) and reactive oxygen species (ROS). Evidence now suggests ROS-mediated damage to sperm is a significant contributing pathology in 30–80% of cases (Agarwal *et al*. 2006; Tremellen 2008).

Alzheimer's disease (Vergallo *et al.* 2018), cancer (Ma-On *et al.* 2017), heart failure (Li *et al.* 2016) and obesity (Dursun *et al.* 2016) are just a few of the disorders that have been connected to OS's ubiquitous effect in humans. Moreover, roughly 35% of infertile men have OS, making it a common biomarker in their semen. Male reproductive diseases such as varicocele, inflammation and prostate cancer have all been linked to increased levels of seminal ROS (Lanzafame *et al.* 2009; Kurfurstova *et al.* 2016; Nowicka-Bauer and Nixon 2020).

Normal spermatocyte capacitation and acrosome reaction depend on a low concentration of ROS. The concentration of ROS is critical to spermatogenesis and sperm maturation, hence there must be rigorous mechanisms for regulating the amount of ROS inside the male reproductive tract and seminal fluid (Alahmar 2019; Cilio *et al.* 2022).

Thioacetamide (TAA) In place of hydrogen sulfide, thioacetimidic acid/acetothioamide (CH3CSNH2) is a sulfur-containing chemical frequently utilized in healthcare and manufacturing (Al-Attar 2011). TAA is often used to induce liver injury (hepatic necrosis/apoptosis) (Wang *et al.* 2019), hepatic fibrosis (Makled *et al.* 2019) and cirrhosis (Keshk *et al.* 2019). It also affects the cardiovascular, urinary, and nervous systems (Amirtharaj *et al.* 2017; Khiat *et al.* 2019). Although TAA is often used to induce liver damage, it causes damage to the testis (Kang *et al.* 2006; Celik *et al.* 2016; Karabulut *et al.* 2020). Antioxidant enzyme activities have been reported to be decreased in the testes of thioacetamide-induced cirrhotic rats (Abul *et al.* 2002). Therefore, antioxidants may inhibit the production of ROS, allowing for the healing of damaged cells (Lin *et al.* 2015).

The treatment of infertility has evolved through time to incorporate a wide range of methods, from the use of synthetic medications to that of natural goods and supplements (Oyewopo *et al.* 2021). Numerous plant

species contain the flavonoid and antioxidant luteolin (3′, 4′, 5, 7-tetrahydroxyflavone, LUT). Broccoli, pepper, thyme, and celery are just a few of the many fruits and vegetables that naturally contain glycosylated LUT (Al-Megrin *et al.* 2020). Moreover, LUT may powerfully scavenge free radicals, which helps reduce oxidative damage to the biosystem (Ijaz *et al.* 2022). Epidemiological studies have shown that the high consumption of LUT-containing foods can reduce the risks of chronic diseases (Kerimoğlu *et al.* 2016). Antioxidant and anti-inflammatory effects (Wang *et al.* 2020), anticancer (Xu *et al.* 2019) and neuroprotective (Theoharides *et al.* 2016), as well as its ability to inhibit the production of free radicals, are the basis for LUT's pharmacological. In addition, new evidence suggests that Luteolin inhibits systemic and neuroinflammatory reactions in 2019 Coronavirus disease (COVID-19) (Kempuraj *et al.* 2021).

Therefore, in the current study, we established an animal model of testicular toxicity induced by Thioacetamide in male rats. Thioacetamide-induced spermatotoxicity and testicular histopathology were also evaluated, with Luteolin supplementation at high doses. This study was designed to provide a reference for further revealing the hazrad of OS and decreasing the damage with Luteolin supplementation *via* histopathological, morphometrical and biochemical evalaution.

Materials and Methods

Drugs and chemicals

Thioacetamide was used as an inducer of testis damage nad Luteolin (LUT) as an antioxidant substance in the experiment. They were obtained from Sigma Chemical Co., MO, USA.

Experimental animals

Thirty adult male *Wistar albino* rats weighing 180 – 250 g were obtained from King Fahd animal house in Jeddah, Saudi Arabia. The animals were housed in plastic cages (10 animals for each) at a temperature of 25°C and 50–70% humidity, with 12 h light/ dark cycles and were fed a freely standard rodent diet and water.

Ethical approval statement

All the animals received human care according to the standard guidelines. Ethical approval for the study was obtained from the Research Ethics Committee, which is in force at the University of Jeddah. The rats were treated in accordance with the Laboratory Animal Treatment Agreement of the Kingdom of Saudi Arabia and the ethical regulations were followed in accordance with the national and institutional guidelines with the protocol published by the National Institutes of Health.

Experimental design

The rats used in the experiment were randomly divided into three groups (ten animals each) and placed in cages as follow: Negative control group (G1) rats were given 1 mL/kg body weight (BW) normal saline solution (0.9% NaCl) i.p. three times a week at 24 h intervals for four weeks, in addition to 3 mL/kg body BW of normal saline solution orally once a day. Positive control group (G2) rats were injected i.p. with TAA at the dose of (200 mg/kg BW) 3 times weekly at 24 h intervals for four weeks to induce testicular toxicity (Celik *et al.* 2016). TAA + LUT group (G3) rats received Luteolin at a daily dose of (50 mg/kg BW orally) for four weeks (Kalbolandi *et al.* 2019) concurrently with i.p. injection of TAA in the same dose as G2.

Testicular weight measurements

At the end of experiment, the testes was weighed to collect data for statistical analysis.

Sample collection

Twenty-four hours after the last treatment, all animals were were ethically anesthetized by i.p. injection of 40 mg/kg thiopental ether. Testis was excised immediately. Dissected right testes were processed for microscopic examination and stained with different histological and immuno-histochemical stains for mapping Sertoli Cells with an anti-vimentin antibody. In addition, the dissected left testis was prepared for tissue homogenate for biochemical assays. Also, blood samples were collected for sexual hormones assays.

Biochemical studies

Determination of sexual hormones

Blood was collected from the retro-orbital veins in which 3 cm of blood into a plain tube was taken and centrifuged at 3000 rpm at 4°C for 5 min to get the serum. The separated sera were used for the estimation of serum levels of testosterone hormone (TH), luteinizing hormone (LH) and follicle-stimulating hormone (FSH). TH serum levels were identified by by enzyme-linked immunosorbent assay (ELISA) according to the instructions of the manufacturer (The BioVendor Mouse /Rat Testosterone). LH and FSH levels in the serum were calculated using ELISA kits per the manufacturer's instructions (Cat.: MBS764675 and MBS2021901, MyBioSource, San Diego, California, United States) ELISA kits for LH and FSH, respectively.

Determination of the testicular oxidative stress status and antioxidant enzymes

The left testis was homogenized from each rat in ice-cold (10% w/v) phosphate-buffered saline (50 m*M* K2HPO4, pH

7.4). The supernatant was separated by centrifugation at 1000 g for 20 min at 4ºC. Antioxidant enzymes such reduced glutathione (GSH), superoxide dismutase (SOD) and catalase (CAT) (Beutler 1963; McCord and Fridovich 1969; Aebi 1984), as well as malondialdehyde (MDA) were measured in the supernatant to determine the level of oxidative stress present (Ohkawa *et al.* 1979). Analyses were made according to the manufacturer's instructions (Cat.: MBS738685, MBS724319, MBS036924 and MBS701908, MyBioSource, San Diego, California, United States) ELISA kits for MDA, GSH, SOD and CAT, respectively. Colorimetric analysis was performed on a homogenate of testes to determine their concentration. Spectrophotometry was used to analyze the concentrations of MDA, GSH, SOD and CAT, which were determined with the help of standard curves. MDA activity was expressed as nmol\mL, GSH as ng\mL, SOD as U/mL and GAT as Mu\L.

Histological and immunohistochemical studies

Histological studies for light microscopy: A 4% buffered formalin solution was used to preserve the right testes for 14 days after they were removed. Tissues were fixed, then dehydrated in a series of graded alcohols, and finally cleaned with xylene. Paraffin was then used to impregnate the samples. Histopathological and immunohistochemical analysis was performed on transverse sections cut with a rotary microtome at a thickness of six micrometers. Hematoxylin and eosin (H & E) stain was used for routine histological examination, whereas Masson trichrome stain was used to identify collagen fibers in histopathological sections (Suvarna *et al.* 2018).

Immunohistochemical study: Deparaffinized, positively charged slide sections (6 µm) embedded in paraffin were soaked in PBS and pretreated with 3% hydrogen peroxide in distilled water to inactivate endogenous peroxidase activity. Antibodies were diluted with 10% normal horse serum (NHS) in phosphate-buffered saline (PBS) (1: 200) before being applied to the sections and incubated overnight with a polyclonal Rabbit anti-goat antibody to Vimentin from Santa Cruz Biotechnology in Dallas, Texas, USA. Finally, the sections were incubated with biotinylated immunoglobulin (1:300, purchased from Boster Biotechnology Co., Ltd., CA, USA) diluted in NHS at 2% for 30 min at room temperature after being washed three times in PBS. After three washes in PBS, the sections were incubated at room temperature for 30 min with peroxidase-conjugated streptavidin diluted in PBS. Finally, the sections were counterstained with Mayers hematoxylin, dried in a sequence of ethanol and xylene, mounted and finally dyed using a diaminobenzidine (DAB) kit (purchased from Boster Bio-Technology Co., Ltd., CA, USA). The positively stained area was brown. A specific primary antibody was switched out for PBS saline as a negative control.

Morphometric analysis

To conduct the morphometric analysis, a plugin for the image analyzer Olympus Image J, NIH, 1.41b, America Inc., Melville, NY, USA was used on tissue samples from all rats in each group (n = 10). In order to get accurate results, we measured five separate slides from each rat in each group. On average, we looked at five distinct fields every slide. Briefly, the average diameter of the testicular seminiferous tubules (H & E X20) was calculated and those tubules were selected which were rounded on the transverse cut. Then, their diameters in two perpendicular directions were measured to determine the average diameter of the seminiferous tubules (Narayana *et al.* 2006). In the case of oblique sections, only the minor axis was considered during the measurement process (Stumpp *et al.* 2004). The average thickness of the germinal epithelium was also measured (using H&E X20). The percentage of collagen fibers in Masson trichrome-stained sections at a magnification of X20 and the percentage of vimentin-positive cells were then calculated as the means (X20).

Statistical Analysis

Data were analyzed using SPSS for Windows (version 26; IBM Corp., Armica, NY, USA). Statistics were summarized by standard deviation of means. One-way analysis of variance followed by a post hoc LSD test was used to assess differences among the groups. $P = 0.05$ was considered significant. Information was presented graphically using GraphPad® Prism 9 (2022), Statistical Package.

Results

Testicular weight measurements

Concerning right and left testis weight, there were highly significant ($P < 0.0001$ and $P < 0.0001$; respectively) increases in negative control G1 as compared to positive control treated G2. Also, significant ($P < 0.01$, $P < 0.0001$ and $P < 0.001$; respectively) increase in body weights (249.0 ± 25.07) , right (1.50 ± 0.17) and left (1.50 ± 0.17) testis weights were detected in G3 (TAA + LUT) as compared to G2 (TAA). Interestingly, there was a non-significant ($P = 0.39$, $P = 0.21$, $P = 0.17$; respectively) difference in G3 (TAA + LUT) regarding rat body weights, right testis weight and left testis weight as compared to a negative control group (G1) (Table 1 and Fig. 1).

Evaluation of sexual hormones

Table 2 and Fig. 2 show different groups' mean ± SD of TH, LH, and FSH levels. Group II (positive control group) showed a highly significant decrease ($P < 0.0001$, $P < 0.0001$ and $P < 0.0001$; respectively) in serum TH (118.6 ± 10.43), LH (0.75 ± 0.12), and FSH (0.95 ± 0.32) compared

Table 1: Testis weight of all experimental groups

Groups	Negative control group (G1)	Positive control group (G2)	TAA + LUT group (G3)	P value
n	10	10	10	
Right testis weight (g)	1.59 ± 0.05	1.22 ± 0.05	1.50 ± 0.17	< 0.0001
		a (****)	a (ns)	0.2110
			b (****)	< 0.0001
Left testis weight (g)	1.60 ± 0.07	1.24 ± 0.06	1.50 ± 0.17	< 0.0001
		a (****)	a (ns)	0.1714
			b (***)	0.0001

Data were presented as mean and standard deviation (Mean ± SD), n= Number of rats /group, a: compared to Negative control group (G1), b: compared to Positive control group (G2), ns = non-significant, ** *P < 0.01*, *** *P < 0.001*, **** *P < 0.0001*. TAA: Thioacetamide. LUT: Luteolin

Table 2: Comparison between all experimental groups according to the levels of Serum testosterone (TS, ng\dL), Serum luteinizing hormone (LH, IU\L), and Serum follicle-stimulating hormone (FSH, IU\L)

Groups	Negative control group (G1)	Positive control group (G2)	TAA + LUT group (G3)	P value
n	10	10	10	
Serum testosterone (TH) (ng\dL)	292.4 ± 29.74	118.6 ± 10.43	270.6 ± 41.38	< 0.0001
		a (****)	a (ns)	0.30
			b (****)	< 0.0001
Serum luteinizing hormone (LH) (IU\L)	4.34 ± 0.66	0.75 ± 0.12	3.96 ± 1.85	< 0.0001
		a (****)	a (ns)	0.84
			b (****)	< 0.0001
Serum follicle-stimulating hormone (FSH) (IU\L)	4.80 ± 1.01	0.95 ± 0.32	4.72 ± 0.85	< 0.0001
		a (****)	a (ns)	0.99
			b (****)	< 0.0001

Data were presented as mean and standard deviation (Mean ± SD), n= Number of rats /group, a: compared to Negative control group (G1), b: compared to Positive control group (G2), ns= non-significant, **** *P < 0.0001*. TAA: Thioacetamide. LUT: Luteolin

Table 3: Comparison between all experimental groups according to the levels of oxidative stress enzyme malondialdehyde (MDA, nmol\mL) and the antioxidant enzymes such as reduced glutathione (GSH, ng\mL), superoxide dismutase (SOD, μ\mL), and catalase (CAT, Mu\L) in testis tissue homogenate

Groups	Negative control group (G1)	Positive control group (G2)	TAA + LUT group (G3)	P value
n	10	10	10	
Malondialdehyde (MDA, nmol\mL)	0.37 ± 0.10	1.45 ± 0.09	0.56 ± 0.20	< 0.0001
		a (****)	a (*)	0.01
			b (****)	< 0.0001
Reduced glutathione (GSH, ng\mL)	16.12 ± 2.32	2.18 ± 0.67	16.12 ± 2.29	< 0.0001
		a (****)	a (ns)	> 0.99
			b (****)	< 0.0001
Superoxide dismutase (SOD, μ\mL)	170.40 ± 9.34	79.60 ± 18.96	163.2 ± 12.53	< 0.0001
		a (****)	a (ns)	0.60
			b (****)	< 0.0001
Catalase (CAT, MU\L)	112.2 ± 4.96	55.40 ± 11.52	117.6 ± 1.95	< 0.0001
		a (****)	a (ns)	0.29
			b (****)	< 0.0001

Data were presented as mean and standard deviation (Mean ± SD), n= Number of rats /group, a: compared to Negative control group (G1), b: compared to Positive control group (G2), ns = non-significant, **** *P < 0.0001*. TAA: Thioacetamide. LUT: Luteolin

with the negative control group (292.4 ± 29.74, 4.34 ± 0.66, 4.80 ± 1.01; respectively) and TAA + LUT treated group (270.6 ± 41.38, 3.96 ± 1.85, 4.72 ± 0.85; respectively). Whereas G3 (TAA + LUT treated rats) showed a highly significant (*P < 0.0001*, *P < 0.0001* and *P < 0.0001*; respectively) increased serum TH, LH, and FSH versus the G2 (positive control group). Meanwhile, G3 showed a non-significant difference in serum TH, LH, and FSH levels (*P* = 0.30, 0.84, 0.99, respectively) compared with the negative control group (G1).

Evaluation of the testicular oxidative stress status and antioxidant enzymes

MDA and antioxidants markers GSH, SOD and CAT, were expressed as mean ± SD in all experimental groups (Table 3 and Fig. 3). The mean value of the MDA level demonstrated a significant increase (1.45 ± 0.09, *P < 0.0001*). In contrast, a significant reduction (*P < 0.0001*) in the levels of antioxidant markers such as GSH (2.18 ± 0.67), SOD (79.60 ± 18.96) and CAT (55.40 ± 11.52) were seen in rats of G2 versus G1 and TAA + LUT group (G3). There were no significant changes (*P > 0.99*, *P* = 0.60, *P* = 0.29; respectively) detected in the levels of GSH, SOD and CAT in TAA + LUT group (G3) (16.12 ± 2.29, 163.2 ± 12.53, 117.6 ± 1.95; respectively) as compared to the negative control group (16.12 ± 2.32, 170.40 ± 9.34, 112.2 ± 4.96; respectively). While there was a significant increase in the MDA level (0.56 ± 0.20, *P* = 0.01) in G3 compared to the MDA level (0.37 ± 0.10) in G1.

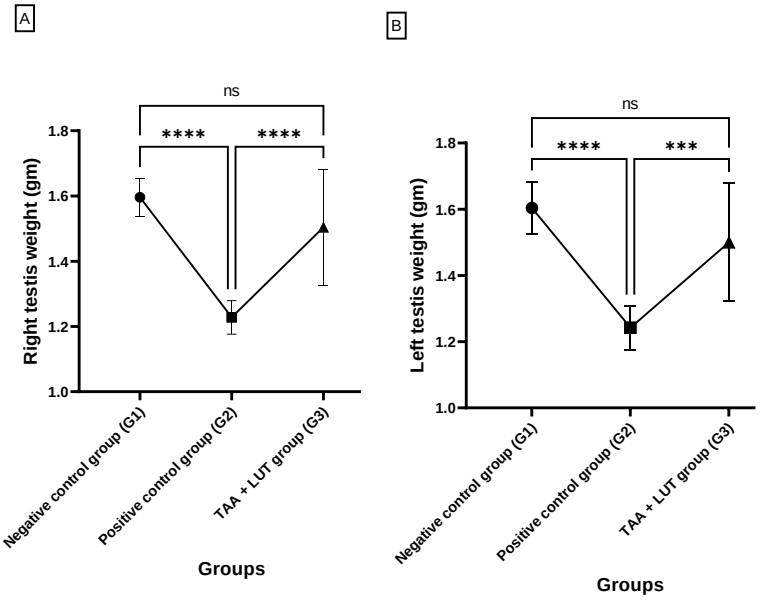

Fig. 1: Chart showing: (**A**) Right testis weight (g), and (**B**) Left testis weight (g) among all experimental groups after the administration of Thioacetamide (TAA) and Luteolin (LUT). Data were presented as mean and standard deviation (Mean ± SD), ns = non-significant, ** *P < 0.01*, *** *P < 0.001*, **** *P < 0. 0001*

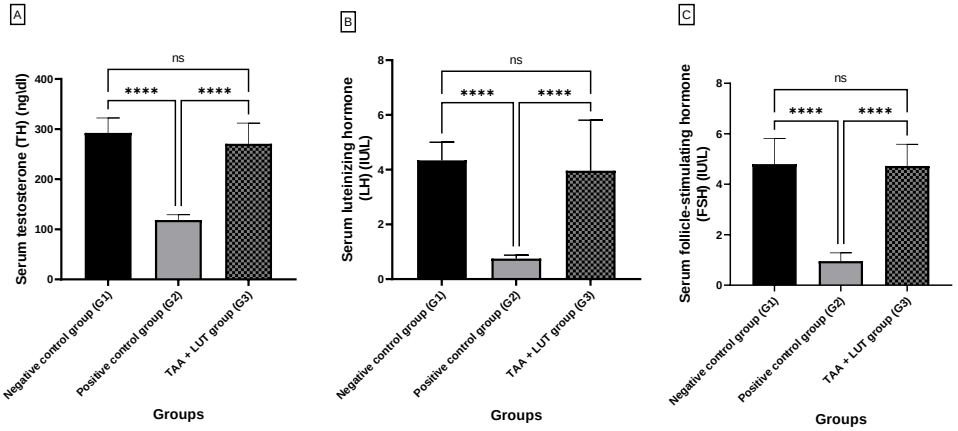

Fig. 2: Chart showing: (**A**) Serum testosterone (TS, ng\dL), (**B**) Serum luteinizing hormone (LH, IU\L), and (**C**) Serum follicle-stimulating hormone (FSH, IU\L) among all experimental groups after the administration of Thioacetamide (TAA) and Luteolin (LUT). Data were presented as mean and standard deviation (Mean ± SD), ns= non-significant, **** *P < 0. 0001*

Histological results

H & E results: Examination of H& E stained sections from negative control group (G1) testis showed normal histological architecture. Clusters of interstitial Leydig cells with acidophilic cytoplasm and vesicular nuclei were seen in the interstitial spaces between the firmly packed seminiferous tubules in the testicular tissue. Each seminiferous tubule had a distinct basement membrane and was lined by myoid cells with flat nuclei. Semineferous tubules bordered with Sertoli cells and stratified germinal epithelium. The germinal epithelium is formed of spermatogonia, primary spermatocytes, early and late spermatids and sperms. Spermatogonia appeared as small rounded cells with rounded nuclei present in the basal part of the tubules. Primary spermatocytes were larger in size than spermatogonia with large rounded nuclei. Early spermatids appeared as small rounded cells with paler nuclei. Sperms were demonstrated by their long tails in the lumen of tubules. The Sertoli cells established a pyramidal shape between the spermatogenic cells and a smooth basement membrane. They had large pale vesicular nuclei and prominent nucleoli. Even spermatozoa could be seen in the seminiferous tubules lumen (Fig. 4).

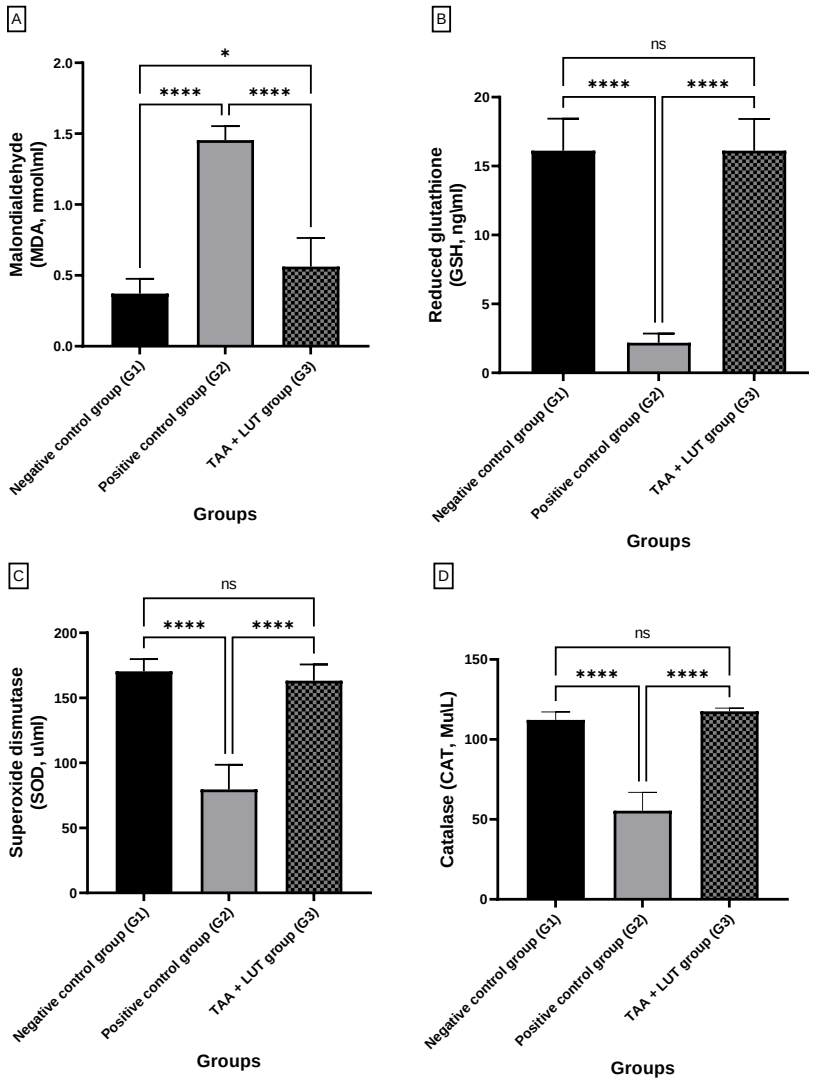

Fig. 3: Chart showing: (**A**) Malondialdehyde (MDA, nmol\ml) and the antioxidant enzymes such as (**B**) Reduced glutathione (GSH, ng\mL), (**C**) Superoxide dismutase (SOD, μ\mL), and (**D**) Catalase (CAT, MU\L) in testis tissue homogenate among all experimental groups after the administration of Thioacetamide (TAA) and Luteolin (LUT). Data were presented as mean and standard deviation (Mean ± SD), ns = non-significant, * $P < 0.05$, **** $P < 0.0001$

In the positive control group (G2) (Fig. 5), impairment of normal architecture of testicular tissue with wide interstitial spaces between tubules and arrested spermatocytes in a different stage in the division was seen. Sloughing of the basal lamina of many seminiferous tubules from lamina propria, loss of stratal arrangement of germinal epithelium with wide intercellular separation, occluded lumen with vacuolated eosinophilic substance and wide interstitial space filled with eosinophilic material. The Sertoli cell showed pale nuclei, distorted and destructed cytoplasmic extension, few elongated spermatids and round spermatids, and few flagella of mature sperms in lumina. Wide interstitial spaces had Leydig cells, dilated congested blood vessels between seminiferous tubules and eosinophilic material. Germinal epithelium seemed thinner, spermatogenic cells appeared deformed and their nuclei were apaptotoic, and there were large gaps between spermatogenic cells. The absence of sperms inside the lumen of seminiferous tubules was also noticed.

However, TAA + LUT treated group (G3) showed normal seminiferous tubules surrounded by a basement membrane lined by Sertoli cells and stratified germinal epithelium. Spermatogonia rested on the basal lamina and was closely related with little intercellular spacing. Spermatids in various stages of spermiogenesis were present as rounded spermatids, and elongated spermatids embedded in cytoplasmic extensions of Sertoli cells were seen. Sperms were observed in the seminiferous tubules lumen. Leydig cells were noticed in the normal interstitial tissue (Fig. 6).

Masson trichrome stained sections: Collagen fibers in the

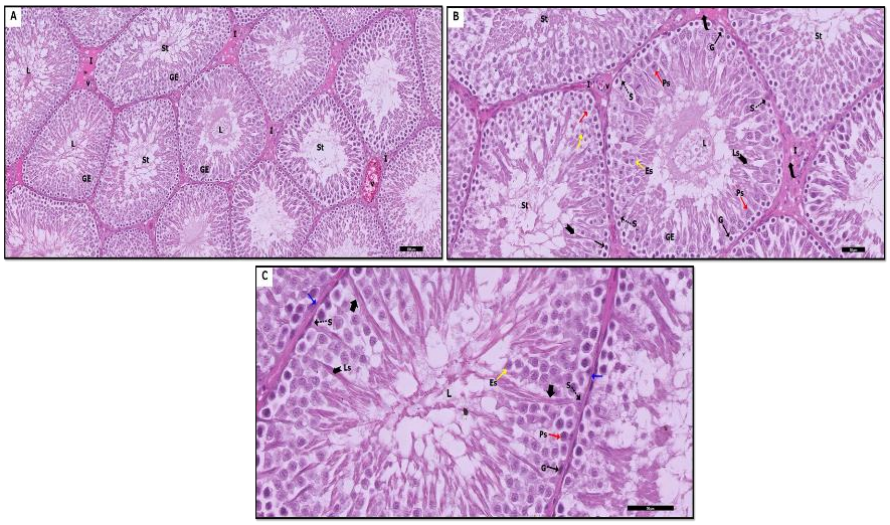

Fig. 4: Testicular sections of adult male rats in the negative control group (G1) showing:
(A) Normal testicular architecture of seminiferous tubules (St). The regular arrangement of closely packed seminiferous tubules (St). Multiple seminiferous tubules (St) with regular outlines, lined by stratified germinal epithelium (GE) and lumen (L) filled with sperm flagella. Clusters of Interstitial cells of Leydig (curved arrow) with acidophilic cytoplasm and vesicular nuclei around blood vessels (v) in the interstitial spaces (I) in-between tubules. (H&E stain X 100, scale bar 100 μm)
(B) Each seminiferous tubule (St) is lined by Sertoli cells (S) and stratified germinal epithelium (GE). Each seminiferous tubule is surrounded by a well-defined basement membrane and flattened myoid cells (blue arrow) with flattened nuclei. GE is formed of spermatogonia (G), primary spermatocytes (Ps), early (Es) and late spermatids (Ls), and lumen (L) filled with sperm flagella. (H&E stain X 20, scale bar 50 μm)
(C) Spermatogonium (G) small, rounded cells with rounded nuclei resting on the basement membrane, primary spermatocyte (Ps) larger rounded cells with large, rounded nuclei, early spermatids (Rs) small, rounded cells with paler nuclei, and many elongated spermatids (Ls) are detected. Sertoli cell (S) appears with a vesicular nucleus and a well-formed cytoplasmic extension (arrowhead). (H&E stain X 40, scale bar 50 μm)

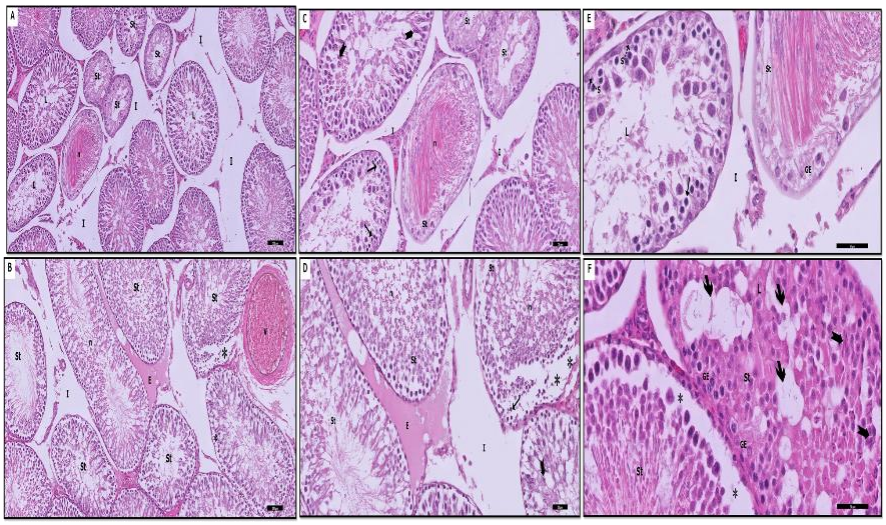

Fig. 5: Testicular sections of adult male rats in the positive control group (G2) show:
(A) loss of normal architecture of testicular tissue with wide interstitial spaces (I) between tubules and arrested spermatocytes in a different stage in the division are seen. Many other tubules (St) are depleted of most of the spermatogenic cells. Note, occluded lumen (L) with remnants of spermatogenic cells(n). (H&E stain X 100, scale bar 100 μm)
(B) another section shows the sloughing of the basal lamina of many seminiferous tubules (St) from lamina propria (*) and wide interstitial (I) spaces filled with eosinophilic material (E) and dilated congested blood vessel (V). The absence of sperms inside the lumen of seminiferous tubules (St) is sometimes noticed and other lumens fill with remanent of spermatogenic cells (n). (H&E stain X 100, scale bar 100 μm)
(C) Severely affected tubules (St) with extensive loss of their germinal epithelium. Note, occluded lumen with remnants of spermatogenic cells(n). Distorted tubules with deeply stained pyknotic nuclei of germinal epithelium (↑) and a few elongated spermatids (bifid arrow) are also noticed. (H&E stain X 20, scale bar 50 μm)
(D) Sloughing of the basal lamina of many seminiferous tubules (St) from lamina propria, loss of stratal arrangement of germinal epithelium with wide intercellular separation (*), occluded lumen with remanent of spermatogenic cells (n). Distorted tubules with deeply stained pyknotic nuclei of germinal epithelium (↑) and a few elongated spermatids (bifid arrow) are seen. Wide interstitial spaces (I) filled with eosinophilic material (E) are also noticed. (H&E stain X 20, scale bar 50 μm)
(E) higher magnification of shows wide intercellular separation. Sloughing of the basal lamina of many seminiferous tubules (St) from lamina propria (*) and wide interstitial space (I). Some Sertoli cells (S) appear with pale nuclei and destructed cytoplasmic extension. Note, occluded lumen (L) with vacuolated eosinophilic substance (n). Sloughing of the basal lamina of many seminiferous tubules (St) from lamina propria (*) and wide interstitial space (I). (H&E stain X 40, scale bar 50 μm)
higher magnification shows part of a seminiferous tubule (St) with distorted germ cells, spermatogonia (↑) have oval dark stained nuclei and Sertoli cell (S) with a pale nucleus and destructed cytoplasmic extensions with wide interstitial spaces (I) between tubules. Note, a seminiferous tubule (St) with extensive loss of germinal epithelium (GE). (H&E stain X 40, scale bar 50 μm)

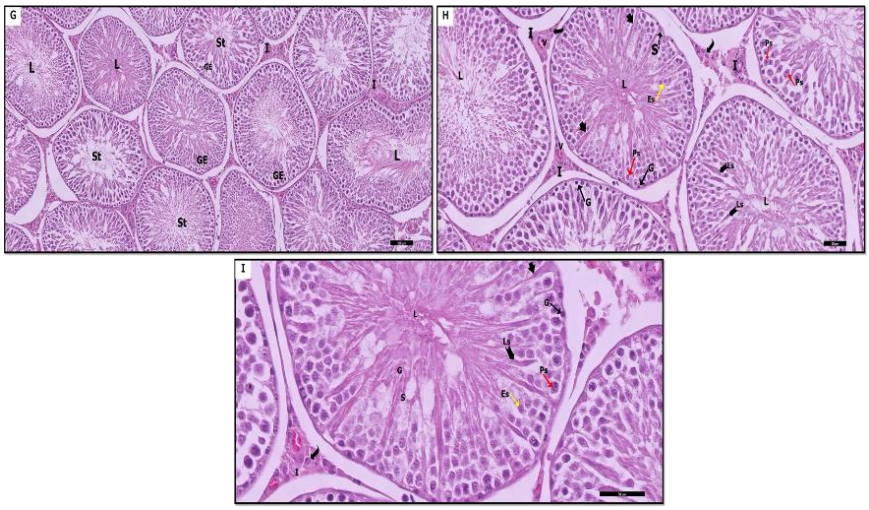

Fig. 6: Testicular sections of adult male rats in TAA+LUT treated group (G3) showing:
(A) Normal testicular architecture of seminiferous tubules (St). The regular arrangement of closely packed seminiferous tubules (St). Multiple seminiferous tubules (St) with regular outlines, lined by stratified germinal epithelium (GE) and lumen (L) filled with sperm flagella. Clusters of Interstitial cells of Leydig (curved arrow) with acidophilic cytoplasm and vesicular nuclei around blood vessels (v) in the interstitium (I) in-between tubules. (H&E stain X 100, scale bar 100 μm)
(B) Each seminiferous tubule (St) is lined by Sertoli cells (S) and stratified germinal epithelium (GE). Each seminiferous tubule is surrounded by a well-defined basement membrane and flattened myoid cells (blue arrow) with flattened nuclei. GE is formed of spermatogonia (G), primary spermatocytes (Ps), early (Es) and late spermatids (Ls), and lumen (L) filled with sperm flagella. (H&E stain X 20, scale bar 50 μm)
(C) Spermatogonium (G) small, rounded cells with rounded nuclei resting on the basement membrane, primary spermatocyte (Ps) larger rounded cells with large, rounded nuclei, early spermatids (Rs) small, rounded cells with paler nuclei, and many elongated spermatids (Ls) are detected. Sertoli cell (S) appears with a vesicular nucleus and a well-formed cytoplasmic extension (arrowhead). (H&E stain X 40, scale bar 50 μm)

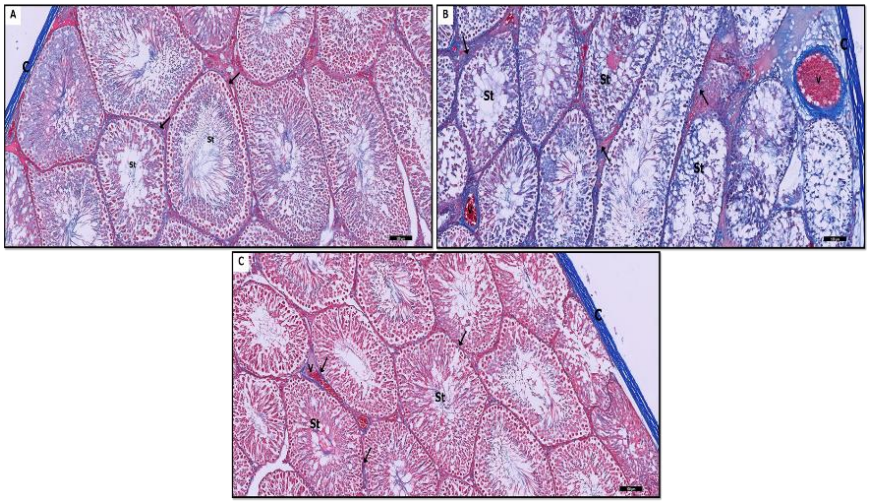

Fig. 7: Testicular sections of adult male rats in
(A) Negative control group (G1) shows a normal distribution of collagen fibers (↑) in capsule (C), and in the basal lamina of seminiferous tubules (St).
(B) Positive control group (G2) shows a marked increase of collagen fibers (↑) in capsule (C), basal lamina of seminiferous tubules (white arrows) and in the wall of blood vessels (V).
(C) TAA+LUT treated group (G3) shows the decreased distribution of collagen fibers (↑) in capsule (C), basal lamina of seminiferous tubules (St) and in the wall of blood vessels (V). Masson trichrome stain (X 100, scale bar 100 µm)

tunica albuginea, basal lamina of the seminiferous tubules, and vessel walls were uniformly distributed in rat testes stained with Masson's trichrome of negative control (Fig. 7A). Increased collagen fibers were found in the testicular capsules, vessel walls and seminiferous tubule basal lamina of the positive control group (Fig. 7B). Collagen fiber distribution was nearly normal in the TAA+LUT treated group compared to G1 (Fig. 7C).

Immunohistochemical reaction results

Midportion and apices of Sertoli cells were immunostained positively for vimentin in G1 as well as their walls with adjoining germ cells and spermatozoa (Fig. 8A_B).

Weak vimentin immunoreaction, in the form of streaks, was observed in G2 at Sertoli-spermatocyte contact points. In addition, the presence of large vacuoles in the

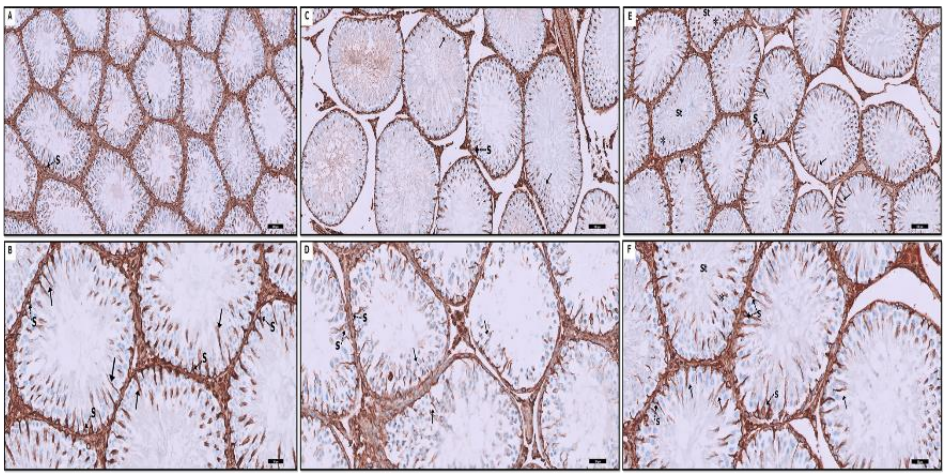

Fig. 8: Testicular sections of adult male rats in
(**A** & **B**) The negative control group (G1) shows the appearance of Sertoli (S) vimentin filaments (immunohistochemical staining), Sertoli cell (S) has perinuclear positivity (dot arrow) and in cytoplasmic extensions (↑).
(**C** & **D**) The positive control group (G2) shows a marked decrease in the number of Sertoli cells (S) with distorted perinuclear positive reaction (dot arrow) and fragmentation of cytoplasmic extensions (↑) irregular basal lamina (curved arrows).
(**E** & **F**) TAA+LUT treated group (G3) shows an apparent increase of positively stained Sertoli cells (S), perinuclear positivity (dot arrow), continuously extended positive cytoplasmic extensions (↑), and few seminiferous tubules (St) appear with fragmented cytoplasmic reaction (*). Vimentin immunohistochemistry (X 100, 200, scale bar 100, 50 μm)

place of degraded spermatocytes was observed in several seminiferous tubules, as evidenced by vimentin immunostaining in those sections. At the same time, mild immunoreactivity was seen in the interstitial cells. G2 showed that the number of Sertoli cells presenting positive vimentin reaction was reduced with disturbed apical cytoplasmic extensions and marked irregularity of the seminiferous tubule basement membrane (Fig. 8C–D).

In TAA and LUT treated group, vimentin filaments' positive reaction within Sertoli cells was concentrated around the nucleus (perinuclear) in the basal part of the cell, then radiating apically toward the apical part of the cell. In addition, a regular basement membrane of the seminiferous tubule was detected. Moreover, the number of Sertoli cells presenting positive vimentin reaction was apparently increased and normally distributed vimentin filaments with cytoplasmic extensions. (Fig. 8E–F).

Morphometrical results

There was a significant difference in the TAA+LUT group in the mean diameter of the seminiferous tubules, the mean germinal epithelial thickness, mean area (%) of collagen fibers content in Masson trichrome stained sections and mean area (%) of vimentin-positive cells (Table 4; Fig. 9).

The mean diameter of the seminiferous tubules was measured and G2 had a significantly decreased mean diameter (163.7 ± 43.16) versus G1 (414.7 ± 54.50) and the TAA + LUT group (454.6 ±27.90) ($P < 0.0001$). However, when comparing the TAA+LUT group to the negative control group, there was a little but non-significant rise (P = 0.13) (Table 4; Fig. 9A).

Regarding the mean germinal epithelial thickness, there was a highly significant ($P < 0.0001$) decrease in the mean germinal epithelial thickness in the positive control group (46.98 ± 4.77) in comparison with both control (74.55 ± 3.10) and TAA+LUT (72.29 ± 4.20) groups. In contrast, there was a non-significant (P = 0.53) increase in the TAA+LUT group compared to the negative control group (Table 4, Fig. 9B).

In the Masson trichrome staining of tissue sections, the positive control group had a significantly higher mean area percent of collagen fibers content (20.55 ± 1.75) than the control (8.72 ± 0.98) and TAA+LUT (10.00 ± 0.3) groups ($P < 0.0001$). While the TAA+LUT group showed a slight increase relative to the negative control group. There was no statistically significant difference (P = 0.065) between the two groups. (Table 4, Fig. 9C).

Comparing the area percent of vimentin-positive staining between the control (15.38 ± 0.48) and TAA+LUT (15.71 ± 0.69) groups, we find that the positive control group shows a statistically significant ($P < 0.0001$) reduction in area percent (11.57 ± 0.24) compared to both control and TAA+LUT groups. Additionally, the TAA+LUT group did not significantly change from the negative control group (P = 0.4017) (Table 4, Fig. 9D).

Discussion

Chemicals and diseases can alter physiological and biochemical activities that impact a man's reproduction ability. Classical qualitative chemical analysis frequently uses. Thioacetamide as an in situ source for sulfide ions; nevertheless, it is harmful to the liver in experimental animal models of exposure (Czechowska *et al.* 2015; Lebda *et al.* 2018). The literature contains only a small number of papers

Table 4: Morphometric analysis in all experimental groups according to the mean diameter of seminiferous tubules (mm), mean thickness of germinal epithelium (μm), mean area % of collagen fibers content in Masson trichrome stained sections (%), and Mean area % of vimentin-positive cells (%)

Groups	Negative control group (G1)	Positive control group (G2)	TAA + LUT group (G3)	P value
n	10	10	10	
Mean diameter of seminiferous tubules (μm)	414.7 ± 54.50	163.7 ± 43.16	454.6 ± 27.90	< 0.0001
		a (****)	a (ns)	0.1398
			b (****)	< 0.0001
Mean thickness of germinal epithelium (μm)	74.55 ± 3.10	46.98 ± 4.77	72.29 ± 4.20	< 0.0001
		a (****)	a (ns)	0.53
			b (****)	< 0.0001
Mean area % of collagen fibres content in Masson trichrome stained sections (%)	8.72 ± 0.98	20.55 ± 1.75	10.00 ± 0.30	< 0.0001
		a (****)	a (ns)	0.0650
			b (****)	< 0.0001
Mean area % of vimentin-positive cells (%)	15.38 ± 0.48	11.57 ± 0.24	15.71 ± 0.69	< 0.0001
		a (****)	a (ns)	0.4017
			b (****)	< 0.0001

Data were presented as mean and standard deviation (Mean ± SD), n = Number of rats /group, a: compared to Negative control group (G1), b: compared to Positive control group (G2), ns = non-significant, **** *P < 0.0001*. TAA: Thioacetamide. LUT: Luteolin

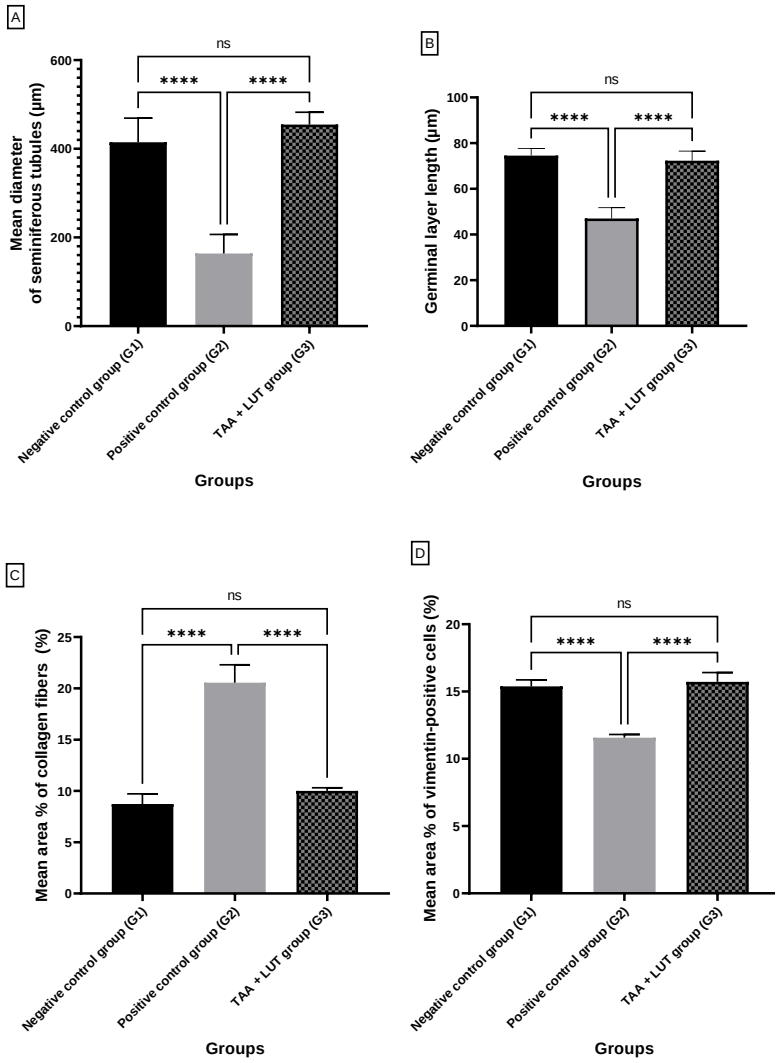

Fig. 9: Chart showing: **(A)** the mean diameter of seminiferous tubules (mm), (**B**) mean thickness of germinal epithelium (μm), (**C**) mean area % of collagen fibers content in Masson trichrome stained sections (%) and (**D**) Mean area % of vimentin-positive cells (%). Data were presented as mean and standard deviation (Mean ± SD), ns = non-significant, **** *P < 0. 0001*

mentioning TAA concerning its effects on the testes. Due to the current buzz surrounding the potential health benefits of herbal remedies and nutritional supplements, this research is particularly timely. The antioxidant, anti-inflammatory, anti-carcinogenic, neuroprotective, and antineoplastic effects of LUT are well-documented (Manju *et al.* 2005).

In the current study, there were statistically significant decreases in right testis weight, and left testis weight in G2 versus G1. These findings corroborate previous studies that TAA exposure significantly altered animals, notably reducing the testicular weight of male rats (Nourozi and Shariati 2020). Testicular weight was also significantly different between TAA-treated and control rats, which may be attributable to the atrophy of the germinal epithelium observed in prior studies following TAA treatment (Celik *et al.* 2016; Lebda *et al.* 2018; Nourozi and Shariati 2020). In addition, Explained that the reduced weight of the testes due to decreases in androgen levels (Elmallah *et al.* 2017). In addition, we discovered that weight loss was lessened in the TAA + LUT group compared to G2, indicating a beneficial impact for LUT.

Spermatogenesis is known to be regulated in great portion by gonadotropins and testosterone (Johnston *et al.* 2004; An *et al.* 2020; Behairy *et al.* 2020). Testosterone and FSH work together to produce sperm in men. There is evidence that both FSH and testosterone stimulate each stage of spermatogenesis (Oduwole *et al.* 2018). LH stimulates testosterone production and secretion by Leydig cells, while FSH acts directly on the seminiferous tubules (MacLachlan *et al.* 2002; Spaliviero *et al.* 2004). In the present study, the serum testosterone level was significantly decreased in G2 (testicular toxicity rat model induced by TAA). A significant decrease in LH and FSH concentration was also noted. Studies have shown that LH, which is generated by the pituitary, stimulates TH production in the male testes. Testosterone levels change dramatically during the life cycle of males (An *et al.* 2020; Kamińska *et al.* 2020; Albasher *et al.* 2021). Found that high OS reduced levels of essential enzymatic and non-enzymatic antioxidants in Leydig cells, leading to a decrease in TH release, which may explain this phenomenon (Cao *et al.* 2004). The reduction in testosterone and LH levels, according to is attributed to the failure of LH binding sites in the body's Leydig cells (El-Sayed and El-Neweshy 2010). There may have been a decrease in the total quantity of spermatids and testosterone, as indicated by Cormier and his coworkers. They also noted that testis weight is directly related to testis function (Cormier *et al.* 2018). Moreover, the current study showed a significant increase in testosterone, LH, and FSH concentration in TAA+LUT treated rats. These results agree with those of in rats pretreated with LUT in lead-induced testicular toxicity. The observed increase in plasma levels suggests that these effects are due to the antioxidant effect of LUT and its metal chelating activity; LUT binds with lead and decreases its toxic effect (Al-Megrin *et al.* 2020).

There has been speculation that oxidative damage is responsible for the observed testicular damage after TAA exposure. Oxidative stress results when there is a discrepancy between the generation and clearance of ROS and free radicals, TAA-induced lipid peroxidation, and the activity of enzymes that prevent oxidative damage is reduced (Celik *et al.* 2016). TAA also generated many ROS, which could interfere with the antioxidant defense system. The overproduction of ROS was harmful to several parts of the cell (Türkmen *et al.* 2022). When ROS peroxidizes fatty acids, indicators of lipid peroxidation, such as MDA, are formed, leading to permanent cell damage and a decrease in the efficacy of the antioxidant defense system, including SOD and CAT activity and GSH levels. Because of their large concentration of polyunsaturated membrane lipids cells equipped with an antioxidant mechanism, the testes are the principal target organs for OS (Sedha *et al.* 2015). Our data demonstrated that TAA exposure promoted lipid peroxidation as measured by a rise in MDA levels and weakened the antioxidant defense system as measured by a decrease in CAT, SOD activity, and GSH. Prior research has demonstrated that TAA causes serious oxidative damage to liver tissue, but there has been considerably less investigation into the effects of TAA on testicles. These research are in agreement with our findings (Czechowska *et al.* 2015; Celik *et al.* 2016; Karabulut *et al.* 2020). Our results show that LUT protects rat testes homogenate from TAA-induced oxidative stress by bolstering the rats' antioxidant defenses. Similarly, Showed that the antioxidant Luteolin significantly mitigated the harmful effects of electromagnetic fields (Yahyazadeh and Altunkaynak 2019).

Histological analysis of TAA-treated rats revealed progressive degeneration of the germinal epithelium lining most of the seminiferous tubules. Other researchers have found similar results, describing the TAA-induced cell death as a "washed out" appearance (Celik *et al.* 2016). The present study found that the testicular tissue architecture in the positive control group showed many forms of abnormalities as vacuolations. Some seminiferous tubules were sloughed from lamina propria, had an irregular outline and were filled with remnants of germinal epithelium. Interstitial tissue was wide, containing eosinophilic exudate, and dilated congested blood vessels. Such an observation is a hallmark of testicular toxicants such as Lead (Albasher *et al.* 2021). Other seminiferous tubules with discarded germinal epithelium from the basal lamina showed darkly stained, apoptotic nuclei of spermatogenic cells. Also, distorted tubules with wide and empty lumina were detected. These were in agreement with Johnson, who explained the destruction of testicular tissue and subsequent infertility by Sertoli cell fragmentation, which provides support and nutrition for the spermatic cells, so its destruction results in the loss of spermatic cells (Johnson 2014). We also found that the lack of intimate interaction of spermatogenic cells may impair proper spermatogenesis, as seen in the high power results. This was characteristic of seminiferous tubule

degeneration as evidenced by degenerating spermatids and a few germinal epithelial cells in tubular lumens. Reported that the close relationship between germ cells and consequently the intercellular bridges was an important landmark of normal spermatogenesis (Lara *et al.* 2018). The use of LUT reduced the severity of the damage, which is in line with previous findings about the potential benefit as a preventative measure (Yahyazadeh and Altunkaynak 2019; Al-Megrin *et al.* 2020).

These histological findings were supported by the current histomorphometric data, which demonstrated a considerable decrease in the diameter and thickness of the germinal epithelium lining the seminiferous tubules in G2 compared to G1. In contrast, we observed that the TAA + LUT group had significantly less damage to the testes. But the significant observation that LUT can minimise the impact of TAA exposure is truly remarkable.

During spermatogenesis, Sertoli cells, which play a crucial role in the formation of germ cells within functional testes, display a range of morphologies (Ahmed *et al.* 2016). The current H&E histopathological findings shows that Sertoli cells were fully mature in the control group (G1) and the TAA + LUT treated group (G3), spermatogenic cells had close relations to each other and Sertoli cytoplasmic extensions, but that these relations had been lost in the G2 group. Sertoli cells make contact with growing germ cells by stretching their cytoplasm. The same was observed in the findings by (Mohammed and Sabry 2020). While in the TAA group, Sertoli cells appeared with destructed cytoplasmic extension, few elongated spermatids, round spermatids and few flagella of mature sperms in lumina. Also, there was an apparent decrease in the Sertoli cells. It has been an archetypal indicator of direct toxicant action on Sertoli cells (Johnson 2014).

Vimentin immunoreactivity was detected in the nucleus and apical area of Sertoli cells, between spermatogonia and primary spermatocytes and in the intercellular spaces between these cell types in G1. Similarly, Reported that in the normal testis, the Sertoli vimentin filaments are either arranged around the nucleus or extend to the apical region of Sertoli cells (Lydka *et al.* 2011). In the positive control group, this immunoreactivity staining diminished. Because vimentin filaments collapsed away from the cell membrane of Sertoli cells, this decrease in vimentin expression harmed testicular tissue. Possible outcomes include Sertoli cell detachment and subsequent apoptosis of detached spermatogenic cells due to lack of nourishment and support (Johnson 2014; Alam *et al.* 2010). Vimentin immunohistochemistry results in Sertoli cells were stronger and apparently increased in the TAA+LUT treated rats compared to the positive control group (testicular toxicity model), suggesting the development of a cytoskeleton that promotes higher mechanical force and the creation of a lengthy sperm nucleus.

These results also imply that intermediate filaments form in a different pattern during late spermatogenesis when they are positioned close to the nucleus of germ cells and that their distribution is highly cyclical during the early stages of the process. Vimentin filaments likewise maintain Sertoli cells' connections with the seminiferous epithelium surrounding spermatogenic cells. Therefore, they are crucial for the completion of spermatogenesis and for gap junction intercellular communication (Show *et al.* 2003; Kopecky *et al.* 2005; ElGhamrawy *et al.* 2014). A considerable drop in the mean area percentage of vimentin-positive cells in the G2 phase was seen in the present morphometric experiments, corroborating the present histology and immunohistochemical findings. Furthermore, their G3 (TAA + LUT) scores improved significantly.

Conclusion

Especially LUT is effective in reducing TAA testicular toxicity by ameliorating histopathological changes and restoring the normal testicular tissue architecture to a great extent, balancing the oxidative tissue state, and increasing gonadotropins and testosterone hormones. Thus, LUT could afford a feasible and useful food-based approach for improving male fertility. Moreover, the Clinical application and therapeutic efficacy of LUT need further investigations and more research to guide its optimal use.

Conflicts of Interest

The authors declare no conflict of interest.

Ethical Approval

All the animals received human care according to the standard guidelines. Ethical approval for the study was obtained from the Research Ethics Committee, which is in force at the University of Jeddah. The rats were treated in accordance with the Laboratory Animal Treatment Agreement of the Kingdom of Saudi Arabia and the ethical regulations were followed in accordance with the national and institutional guidelines with the protocol published by the National Institutes of Health.

References

Abul HT, TC Mathew, F Abul, H Al-Sayer, HM Dashti (2002). Antioxidant enzyme level in the testes of cirrhotic rats. *Nutrition* 18:56–59

Aebi H (1984). Catalase *in vitro*. *In*: *Methods in Enzymology*, Vol. 105, pp:121–126. Elsevier, London

Agarwal A, A Majzoub, N Parekh, R Henkel (2020). A schematic overview of the current status of male infertility practice. *World J Men Health* 38:308–322

Agarwal A, S Gupta, S Sikka (2006). The role of free radicals and antioxidants in reproduction. *Curr Opin Obst Gynecol* 18:325–332

Ahmed N, H Yufei, P Yang, W Muhammad Yasir, Q Zhang, T Liu, C Hong, H Lisi, C Xiaoya, Q Chen (2016). Cytological study on Sertoli cells and their interactions with germ cells during annual reproductive cycle in turtle. *Ecol Evol* 6:4050–4064

Al-Attar AM (2011). Hepatoprotective influence of vitamin C on thioacetamide-induced liver cirrhosis in Wistar male rats. *J Pharmacol Toxicol* 60:218–233

Al-Megrin WA, S Alomar, AF Alkhuriji, DM Metwally, SK Mohamed, RB Kassab, AEA Moneim, MF El-Khadragy (2020). Luteolin protects against testicular injury induced by lead acetate by activating the Nrf2/HO-1 pathway. *IUBMB Life* 72:1787–1798

Alahmar AT (2019). Role of Oxidative Stress in Male Infertility: An Updated Review. *J Hum Reprod Sci* 12:4–18

Alam MS, S Ohsako, TW Tay, N Tsunekawa, Y Kanai, M Kurohmaru (2010). Di (n-butyl) phthalate induces vimentin filaments disruption in rat sertoli cells: A possible relation with spermatogenic cell apoptosis. *Anat Histol Embryol* 39:186–193

Albasher G, R Alrajhi, E Alshammry, R Almeer (2021). *Moringa oleifera* leaf extract attenuates Pb acetate-induced testicular damage in rats. *Combinat Chem High Through Screen* 24:1593–1602

Amirtharaj GJ, SK Natarajan, A Pulimood, KA Balasubramanian, A Venkatraman, A Ramachandran (2017). Role of oxygen free radicals, nitric oxide and mitochondria in mediating cardiac alterations during liver cirrhosis induced by thioacetamide. *Cardiovasc Toxicol* 17:175–184

An Q, K Zhang, L Fu, Y Guo, C Zhang, Z Ge, J Ma, Y Gu, L Zuo (2020). The impact of exogenous testosterone supplementation on spermatogenesis in a rat model of oligoasthenospermia. *Intl J Clin Exp Pathol* 13:1287–1299

Behairy A, NI El-Sharkawy, TM Saber, MM Soliman, MMM Metwally, GI Abd El-Rahman, YM Abd-Elhakim, MME Deib (2020). The modulatory role of vitamin C in boldenone undecylenate induced testicular oxidative damage and androgen receptor dysregulation in adult male rats. *Antioxidants* 9:1053–1068

Beutler E (1963). Improved method for the determination of blood glutathione. *J Lab Clin Med* 61:882–888

Cao L, S Leers-Sucheta, S Azhar (2004). Aging alters the functional expression of enzymatic and non-enzymatic anti-oxidant defense systems in testicular rat Leydig cells. *J Ster Biochem Mol Biol* 88:61–67

Celik H, A Camtosun, O Ciftci, A Cetin, M Aydin, S Gürbüz (2016). Beneficial effects of nerolidol on thioacetamide-induced damage of the reproductive system in male rats. *Biomed Res* 27:725–730

Cilio S, M Rienzo, G Villano, BF Mirto, G Giampaglia, F Capone, G Ferretti, E Di Zazzo, F Crocetto (2022). Beneficial Effects of Antioxidants in Male Infertility Management: A Narrative Review. *Oxygen* 2:1–11

Cormier M, F Ghouili, P Roumaud, W Bauer, M Touaibia, LJ Martin (2018). Influences of flavones on cell viability and cAMP-dependent steroidogenic gene regulation in MA-10 Leydig cells. *Cell Biol Toxicol* 34:23–38

Czechowska G, K Celinski, A Korolczuk, G Wojcicka, J Dudka, A Bojarska, RJ Reiter (2015). Protective effects of melatonin against thioacetamide-induced liver fibrosis in rats. *J Physiol Pharmacol* 66:567–579

Dursun E, FA Akalın, T Genc, N Cinar, O Erel, BO Yildiz (2016). Oxidative stress and periodontal disease in obesity. *Medicine* 95:1–7

El-Sayed YS, MS El-Neweshy (2010). Impact of lead toxicity on male rat reproduction at hormonal and histopathological levels. *Toxicol Environ Chem* 92:765–774

ElGhamrawy TA, D Helmy, HFA Elall (2014). Cadherin and vimentin immunoexpression in the testis of normal and induced infertility models of albino rats. *Fol Morphol* 73:339–346

Elmallah MIY, MF Elkhadragy, EM Al-Olayan, AE Abdel Moneim (2017). Protective effect of *Fragaria ananassa* crude extract on cadmium-induced lipid peroxidation, antioxidant enzymes suppression, and apoptosis in rat testes. *Intl J Mol Sci* 18:957–972

Ijaz MU, F Ayaz, S Mustafa, A Ashraf, MF Albeshr, MN Riaz, S Mahboob (2022). Toxic effect of polyethylene microplastic on testicles and ameliorative effect of luteolin in adult rats: Environmental challenge. *J King Saud Univ Sci* 34:102064

Johnson KJ (2014). Testicular histopathology associated with disruption of the Sertoli cell cytoskeleton. *Spermatogenesis* 4:e979106

Johnston H, PJ Baker, M Abel, HM Charlton, G Jackson, L Fleming, TR Kumar, PJ O'Shaughnessy (2004). Regulation of Sertoli cell number and activity by follicle-stimulating hormone and androgen during postnatal development in the mouse. *Endocrinology* 145:318–329

Kalbolandi SM, AV Gorji, H Babaahmadi-Rezaei, E Mansouri (2019). Luteolin confers renoprotection against ischemia–reperfusion injury *via* involving Nrf2 pathway and regulating miR320. *Mol Biol Rep* 46:4039–4047

Kamińska A, S Marek, L Pardyak, M Brzoskwinia, P Pawlicki, B Bilińska, A Hejmej (2020). Disruption of androgen signaling during puberty affects Notch pathway in rat seminiferous epithelium. *Reprod Biol Endocrinol* 18:1–14

Kang JS, K Morimura, C Toda, H Wanibuchi, M Wei, N Kojima, S Fukushima (2006). Testicular toxicity of DEHP, but not DEHA, is elevated under conditions of thioacetamide-induced liver damage. *Reprod Toxicol* 21:253–259

Karabulut D, AT Akın, M Sayan, E Kaymak, E Ozturk, B Yakan (2020). Effects of melatonin against thioacetamide-induced testicular toxicity in rats. *Intl J Morphol* 38:1455–1462

Kempuraj D, R Thangavel, DD Kempuraj, ME Ahmed, GP Selvakumar, SP Raikwar, SA Zaheer, SS Iyer, R Govindarajan, PN Chandrasekaran (2021). Neuroprotective effects of flavone luteolin in neuroinflammation and neurotrauma. *Biofactors* 47:190–197

Kerimoğlu G, A Aslan, O Baş, S Çolakoğlu, E Odacı (2016). Adverse effects in lumbar spinal cord morphology and tissue biochemistry in Sprague Dawley male rats following exposure to a continuous 1-ha day 900-MHz electromagnetic field throughout adolescence. *J Chem Neuroanat* 78:125–130

Keshk WA, NA Soliman, DA Ali, WS Elseady (2019). Mechanistic evaluation of AMPK/SIRT1/FXR signaling axis, inflammation, and redox status in thioacetamide-induced liver cirrhosis: The role of *Cichorium intybus* Linn (chicory)-supplemented diet. *J Food Biochem* 43:e12938

Khiat AE, L Tamegart, A Draoui, R El Fari, S Sellami, H Rais, O El Hiba, H Gamrani (2019). Kinetic deterioration of short memory in rat with acute hepatic encephalopathy: Involvement of astroglial and neuronal dysfunctions. *Behav Brain Res* 367:201–209

Kopecky M, V Semecky, P Nachtigal (2005). Vimentin expression during altered spermatogenesis in rats. *Acta Histochem* 107:279–289

Kurfurstova D, J Bartkova, R Vrtel, A Mickova, A Burdova, D Majera, M Mistrik, M Kral, FR Santer, J Bouchal (2016). DNA damage signalling barrier, oxidative stress and treatment-relevant DNA repair factor alterations during progression of human prostate cancer. *Mol Oncol* 10:879–894

Lanzafame FM, SL Vignera, E Vicari, AE Calogero (2009). Oxidative stress and medical antioxidant treatment in male infertility. *Reprod Biomed Onl* 19:638–659

Lara NLM, GMJ Costa, GF Avelar, SMSNN Lacerda, RA Hess, LRD França (2018). Testis physiology-overview and histology. In: *Encyclopedia of Reproduction*, pp:105–116. Elseveir, Amsterdam, Netherlands

Lebda MA, KM Sadek, TK Abouzed, HG Tohamy, YS El-Sayed (2018). Melatonin mitigates thioacetamide-induced hepatic fibrosis *via* antioxidant activity and modulation of proinflammatory cytokines and fibrogenic genes. *Life Sci* 192:136–143

Li B, R Chi, F Qin, X Guo (2016). Distinct changes of myocyte autophagy during myocardial hypertrophy and heart failure: Association with oxidative stress. *Exp Physiol* 101:1050–1063

Lin P, X Tian, Y Yi, W Jiang, Y Zhou, W Cheng (2015). Luteolin-induced protection of H_2O_2-induced apoptosis in PC12 cells and the associated pathway. *Mol Med Rep* 12:7699–7704

Lydka M, M Kotula-Balak, I Kopera-Sobota, M Tischner, B Bilińska (2011). Vimentin expression in testes of Arabian stallions. *Equine Vet J* 43:184–189

Ma-On C, A Sanpavat, P Whongsiri, S Suwannasin, N Hirankarn, P Tangkijvanich, C Boonla (2017). Oxidative stress indicated by elevated expression of Nrf2 and 8-OHdG promotes hepatocellular carcinoma progression. *Med Oncol* 34:1–12

MacLachlan RI, L O'Donnell,SJ Meachem, PG Stanton, DMD Kretser, K Pratis, DM Robertson (2002). Identification of specific sites of hormonal regulation in spermatogenesis in rats, monkey, and man. *Rec Progr Horm Res* 57:149–179

Makled MN, MH Sharawy, MS El-Awady (2019). The dual PPAR-α/γ agonist saroglitazar ameliorates thioacetamide-induced liver fibrosis in rats through regulating leptin. *Naunyn-Schmied Arch Pharmacol* 392:1569–1576

Manju V, V Balasubramaniyan, N Nalini (2005). Rat colonic lipid peroxidation and antioxidant status: The effects of dietary luteolin on 1, 2-dimethylhydrazine challenge. *Cell Mol Biol Lett* 10:535–551

McCord JM, I Fridovich (1969). Superoxide dismutase: An enzymic function for erythrocuprein (hemocuprein). *J Biol Chem* 244:6049–6055

Mohammed HO, RM Sabry (2020). The possible role of curcumin against changes caused by paracetamol in testis of adult albino rat (histological, immunohistochemical and biochemical study). *Egypt J Histol* 43:819–834

Narayana K, N Prashanthi, A Nayanatara, LK Bairy, UJA D'SOUZA (2006). An organophosphate insecticide methyl parathion (o-o-dimethyl o-4-nitrophenyl phosphorothioate) induces cytotoxic damage and tubular atrophy in the testis despite elevated testosterone level in the rat. *J Toxicol Sci* 31:177–189

Nourozi A, M Shariati (2020). Protective effect of vitamin D on spermatogenesis and testicular tissue changes in adult rats treated with thioacetamide TT. *Alborz-Health Med J* 9:107–122

Nowicka-Bauer K, B Nixon (2020). Molecular changes induced by oxidative stress that impair human sperm motility. *Antioxidants* 9:134–155

Oduwole OO, H Peltoketo, IT Huhtaniemi (2018). Role of follicle-stimulating hormone in spermatogenesis. *Front Endocrinol* 9:763–773

Ohkawa H, N Ohishi, K Yagi (1979). Assay for lipid peroxides in animal tissues by thiobarbituric acid reaction. *Anal Biochem* 95:351–358

Oyewopo AO, O Adeleke, O Johnson, A Akingbade, KS Olaniyi, ED Areola, O Tokunbo (2021). Regulatory effects of quercetin on testicular histopathology induced by cyanide in Wistar rats. *Heliyon* 7:e07662

Sedha S, S Kumar, S Shukla (2015). Role of oxidative stress in male reproductive dysfunctions with reference to phthalate compounds. *Urol J* 12:2304–2316

Show MD, MD Anway, JS Folmer, BR Zirkin (2003). Reduced intratesticular testosterone concentration alters the polymerization state of the Sertoli cell intermediate filament cytoskeleton by degradation of vimentin. *Endocrinol* 144:5530–5536

Spaliviero JA, M Jimenez, CM Allan, DJ Handelsman (2004). Luteinizing hormone receptor-mediated effects on initiation of spermatogenesis in gonadotropin-deficient (hpg) mice are replicated by testosterone. *Biol Reprod* 70:32–38

Stumpp T, E Sasso-Cerri, E Freymüller, SM Miraglia (2004). *Apoptosis and testicular alterations in albino rats treated with etoposide during the prepubertal phase*, Vol. 279, pp:611–622. The Anatomical Record Part A: Discoveries in Molecular, Cellular, and Evolutionary Biology: An Official Publication of the American Association of Anatomists, Washington DC, USA

Suvarna KS, C Layton, JD Bancroft (2018). *Bancroft's Theory and Practice of Histological Techniques E-Book*. Elsevier Health Sciences, China

Theoharides TC, I Tsilioni, AB Patel, R Doyle (2016). Atopic diseases and inflammation of the brain in the pathogenesis of autism spectrum disorders. *Transl Psych* 6:844–852

Tremellen K (2008). Oxidative stress and male infertility – a clinical perspective. *Hum Reprod Update* 14:243–258

Türkmen NB, H Yüce, A Taşlıdere, Y Şahin, O Çiftçi (2022). The ameliorate effects of nerolidol on thioacetamide-induced oxidative damage in heart and kidney tissue. *Turk J Pharm Sci* 19:1–8

Vergallo A, L Giampietri, F Baldacci, L Volpi, L Chico, C Pagni, FS Giorgi, R Ceravolo, G Tognoni, G Siciliano (2018). Oxidative stress assessment in Alzheimer's disease: A clinic setting study. *Amer J Alzh Dis Dement* 33:35–41

Wang H, H Zhang, Y Wang, L Yang, D Wang (2019). Embelin can protect mice from thioacetamide-induced acute liver injury. *Biomed Pharmacother* 118:109360

Wang S, M Cao, S Xu, J Shi, X Mao, X Yao, C Liu (2020). Luteolin alters macrophage polarization to inhibit inflammation. *Inflammation* 43:95–108

Xu H, BS Linn, Y Zhang, J Ren (2019). A review on the antioxidative and prooxidative properties of luteolin. *React Oxyg Spec* 7:136–147 https://www.scopus.com/inward/record.uri?eid=2-s2.0-85080082895&partnerID=40&md5=5219b461fdd7ddfad2ab5b024ed2fddf

Yahyazadeh A, BZ Altunkaynak (2019). Protective effects of luteolin on rat testis following exposure to 900 MHz electromagnetic field. *Biotech Histochem* 94:298–307